Automatic guiding of the primary image of solar Gregory telescopes

G.Küveler[1], E.Wiehr[2], D.Thomas[1], M.Harzer[1], M.Bianda[3],
A.Epple[4], P.Sütterlin[2], E.Weisshaar[5]

January 28, 1998

1:Fachhochschule Wiesbaden, Am Brückweg 26, D-65428 Rüsselsheim
2:Universitäts-Sternwarte, Geismarlandstr.11, D-37083 Göttingen
3:Istituto Ricerche Solari Locarno, Via Patocchi, CH-6605 Locarno-Monti
4:Max-Planck-Institut für Aeronomie, D-37191 Katlenburg-Lindau
5:Numatec G.m.b.H., D-55262 Heidesheim

Abstract

The primary image reflected from the field-stop of solar Gregory telescopes is used for automatic guiding. This new system avoids temporal varying influences from the bending of the telescope tube by the main mirror's gravity and from offsets between the telescope and a separate guiding refractor. The required stiffness of the guider mechanics and the small areas of the sensors demand small f-numbers for the guider optics, which cause problems with the image quality and with heat. Problems also arise from the imaging of the pinhole in the telescope's field stop. The corresponding lack of image information at that location can be reduced numerically by Fourier methods much more effectively than with profile centering methods. Several types of such guiders are tested, a final equipment, now installed at the Gregory telescopes at Tenerife and at Locarno, is described.

1   Introduction

Automatic guiding is particularly important for solar observations, since a purely hour-driven solar telescope is affected by a number of influences which cause motions of the solar image on the spectrograph slit: (a) the finite accuracy of the alignment of the telescope's polar axis causes a steady image drift; (b) the hour drive introduces quasi-periodical errors from the individual slopes of the teeth in the gear (Soltau & Wiehr 1984); (c) the bending of the telescope tube yields a daily varying shift of the main mirror which exhibits a minimum at noon; (d) the solar declination varies during an

observation up to more than 1"/min at the equinoxes; (e) in the early morning with its usually best seeing conditions, the variation of the atmospheric refraction with altitude above the horizon causes a decreasing error in the apparent hour and declination angles of the sun.

Gregory type telescopes have an elliptically secondary mirror behind the prime focus and thus allow the use of a (water-cooled) field-stop (Ten Bruggenkate & Jäger 1951). The light from the surroundings of the pinhole in this field-stop is often reflected out of the telescope tube without further use, but it can be used for a high precision guiding which may be superior to that of common guiding telescopes. The latter usually remove the influences from daily variations of the solar declination and of the refraction as well as from the finite accuracies of the hour drive and of the alignment of the polar axis, but not those from a bending of the telescope tube. In addition, separate guiding telescopes suffer from a daily varying offset with respect to the main telescope. These effects are be largely reduced using the primary image of a Gregory telescope for guiding. In practice, however, there are several problems with this elegant solution:

- the restricted areas of existing sensors require a small solar image and thus a high mechanical precision in the range of 1μ;

- scanning and positioning of the solar disc on the spectrograph slit should thus not be realized by a mechanical displacement of the sensor;

- a system stiff enough for that precision requires short geometrical lengths and thus a light-path which will be sensitive to optical errors;'

- the enormous heat in the prime focus must be reduced without using optical elements which exhibit (time dependent) disturbances;

- the pinhole in the prime focus field-stop produces a dark dot in the picture of the primary image on the sensor;

2   Modern Sensors

Modern two-dimensional diode sensors have typical areas of $2 \times 2\,\mathrm{cm}^2$ and have been designed for contact-less measurements of small geometric distances using laser spots (e.g. for the alignment of the focusing magnets of particle accelerators). The small amount of information required to determine the X and Y positions is easily handled by a micro processor. First experience with 'lateral effect photo-diodes', LEP, was made at the Locarno telescope (cf. Küveler et al. 1994). However, the LEP's sensitivity to intensity variations (e.g. from varying solar zenith angle) makes it only useful for guiding at a given location on the solar image but not for scanning. In addition, the operation of such a system requires a precise temperature stabilization.
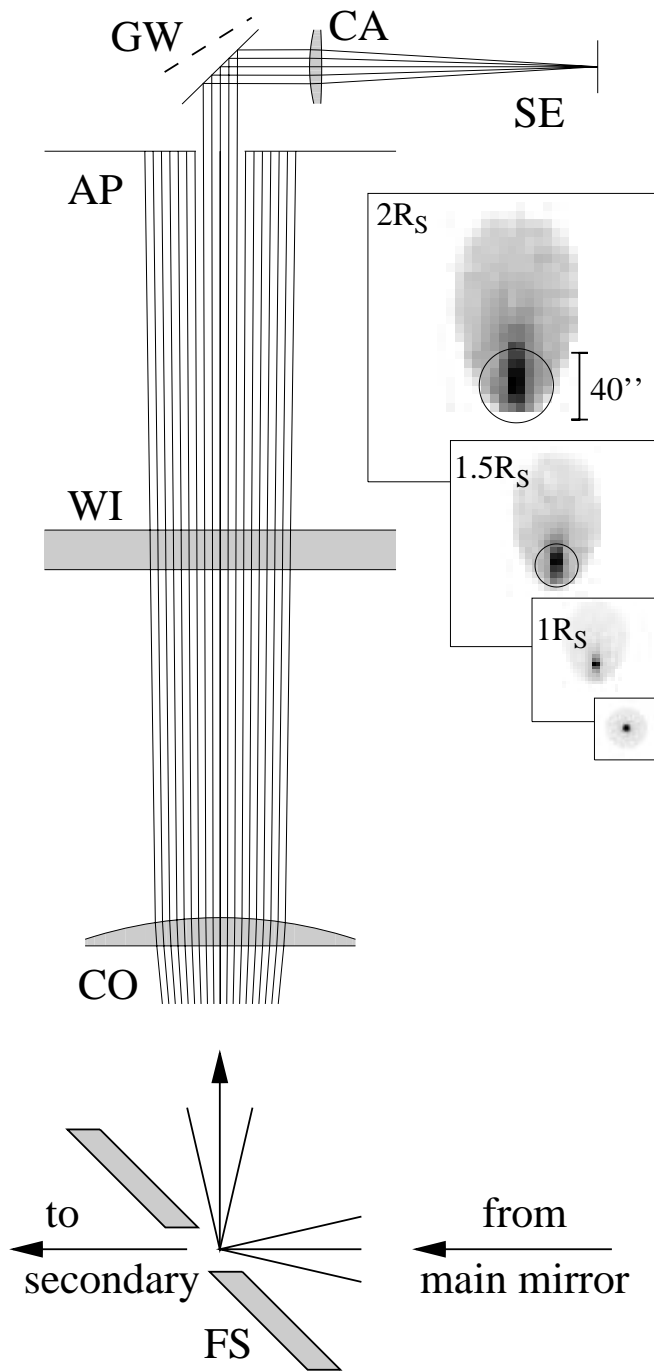
Figure 1: Optical layout of the imaging system for the primary image guider, CO=collimating single lens, WI=window in the vacuum tubus, AP=water-cooled 18 cm aperture in the pupil, GW=glas wedge reflecting 4% of the light intensity, CA=achromatic camera lens, SE=sensor; only schematically indicated is the field stop FS with the Dawe hole. Also given are the spot diagrams, the circles give the 50% energy contour.
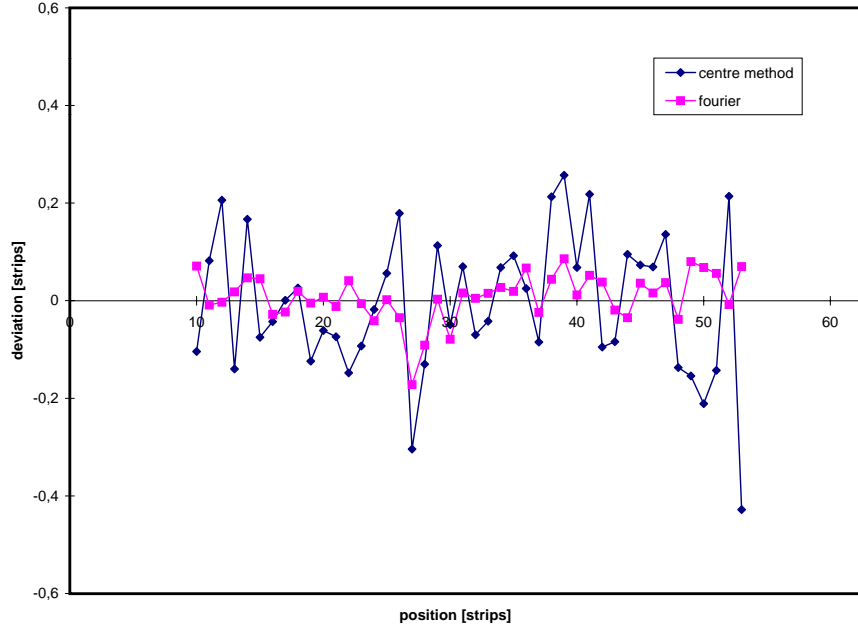
Figure 2: Comparison of the fourier and the center-of-gravity method for a determination of the location of a simultated solar disk profile with 2.5% random noise and a pinhole spanning over three sensor strips reducing the disk intensity by 20%. The disk profile was shifted between strips 10 and 53 in single steps.

We therefore replaced the LEP by a 'digital positioning sensor diode', DPSD, also of $2 \times 2\,\text{cm}^2$ area. This device – available since 1995 – consists of two perpendicular rows with 64 strips in the X and 64 strips in the Y direction. Read-out and data handling of these 128 intensity values is much faster than that of a $64 \cdot 64$ pixel CCD array. Each DPSD row yields one intensity signal which is already internally multiplied by the gain factor, converted, and thus available in digital form. Blum et al. (1995) tested a number of existing sensors and obtained best results for the DPSD produced by 'Heimann'/ Wiesbaden. These sensors are connected to a control module equipped with a 16-bit microprocessor yielding final X, Y positions. The internal center-of-gravity determination of the module is based on simple summing and averaging and turned out to be not sufficient for our purpose. We therefore transmit the original 128 intensity values directly to an external PC which performs the real-time numerical analysis.

4

3 The guider optics

The first of such primary image guiders was installed in 1996 at the Locarno telescope (Brückner et al. 1967). This telescope had been operated since 1970 with a separate (Zeiss) guiding refractor mounted on top of the main telescope tube (Wiehr et al. 1980), and an hourly varying offset with respect to the main telescope introduced drifts of the solar image up to 0.5 arcmin/h on the spectrograph slit. In order to assure a much higher mechanical accuracy of $\approx 1\mu$ for the new guider, the geometrical path has been kept very short. The small f-number required for this layout (cf. Fig.1), introduces optical errors. These, however, turned out to be irrelevant for the accuracy of the guider's 'hold mode'. For the 'scan mode' they can be largely removed by a correction matrix in the computer program.

The light from the reflecting prime focus field-stop is collimated by a $\emptyset = 10$ cm single lens with $f = 30$ cm. It images the telescope's entrance pupil on a water-cooled aperture and assures that the beam passes the $\emptyset = 10$ cm window fixed in the evacuated telescope tube. The optical quality of this window is low since it was not originally fabricated for optical imaging. The beam is then reflected in a direction parallel to the telescope tube by a (4% reflecting) glass plate of $\lambda/20$ accuracy and $4°$ wedge angle avoiding a secondary image from the backside. Although the glass wedge is very close to the pupil image, its metallic holder is not heated since the water-cooled aperture immediately in front reduces the light beam from $\emptyset = 5.5$ cm to $\emptyset = 1.8$ cm. An $f = 10$ cm, $\emptyset = 3.15$ cm achromatic camera lens finally re-images the telescope's primary picture at a $4:1$ reduction on the sensor. The precise intensity adaptation to the sensor's maximum output of 800 counts is made by a 755 nm interference filter 5 cm in front of the sensor; neutral density filters turned out to be too sensitive to temperature variations in connection with displacements of the image.

4 Numerical algorithm

The main problem of determining the solar disc position on the sensor arises from the pinhole in the field-stop which causes a black dot in the solar disc image. This causes the profile to be asymmetric and results in a wrong center-of-profile position. The amount of asymmetry can be defined in the following way: a profile $f(x)$, given as a sample of $2N$ discrete data points like that from our sensor, can be written as a Fourier sequence:

$$f(x) = \sum_{n=-N}^{N} C_k e^{2\pi i k x/N} \tag{1}$$

where $C_k = a_k + ib_k$ are complex Fourier coefficients. If $f(x)$ is symmetric to the origin $x = 0$ the imaginary parts of C_k vanish. In case of a shift Δx from the origin, the term

$$A = \sum_{k=1}^{N} (IM[C_k])^2 \tag{2}$$

can be defined as a measure of asymmetry of function $f(x)$ with respect to $x = 0$. Using the shift theorem for Fourier transforms, equation (2) for an axis shifted by Δx becomes

$$A(\Delta x) = \sum_{k=1}^{N} (IM[C_k e^{-2\pi i k \Delta x/N}])^2 \tag{3}$$

Minimizing A with respect to Δx yields the axis of best symmetry.

The asymmetry introduced by the pinhole may be reduced if the variation problem is extended to $A(\Delta x, f1, f2, f3, \ldots)$, where $f1, f2, f3, \ldots$ are additional variation parameters representing the influence of the pinhole pattern. This method might completely remove the influenece of the pinhole, but it requires more sophisticated numerics, which has to be developed.

As of now, we determine the axis of symmetry by considering only the first Fourier coefficient in (3)

$$IM\left[C_1 e^{-2\pi i \Delta x/N}\right] = a_1 \sin(2\pi \Delta x/N) - b_1 \cdot \cos(2\pi \Delta x/N) = 0 \tag{4}$$

we obtain

$$\Delta x = \frac{N}{2\pi} \arctan\left(\frac{b_1}{a_1}\right) + C \tag{5}$$

The phase correction term C is given in the following table:

b_1	a_1	C
> 0	> 0	0
$*$	< 0	$N/2$
< 0	> 0	N

In the special case $a_1 = 0$ it is $\Delta x = N/4$ if $b_1 > 0$, and $\Delta x = 3N/4$ if $b_1 < 0$.

The evaluation of this formula is quite simple and compares favorably with the center-of-profile method. In a numerical experiments, we first used mathematical profiles without noise, and obtained from both methods nearly the same Δx values. In a second experiment, we simulated a solar intensity profile with a pinhole signal that spans over 3 strips and reduces the intensity by 20% and added random noise of 2.5% of the profile amplitude. The Fourier method (5) three times (rms) better results as from the center-of-profile method (see Fig. 2). The reason is that the latter is very sensitive to noise outside the solar image.
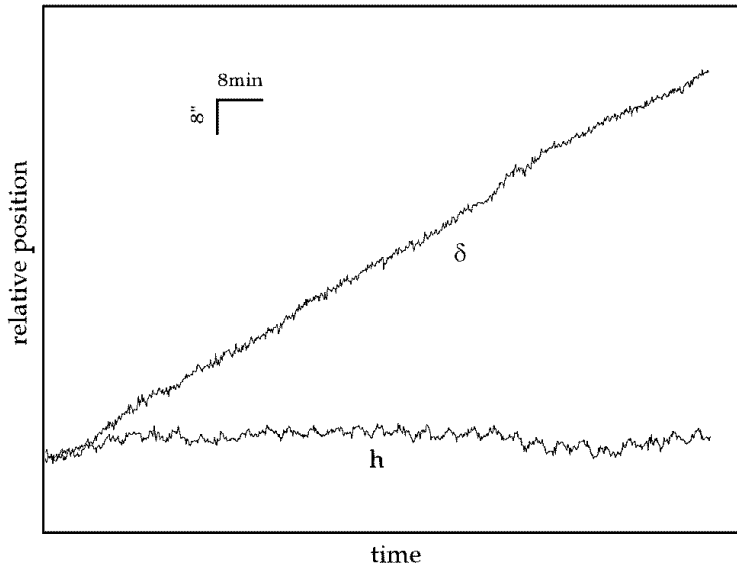
Figure 3: Sensor signals obtained with exclusively hour-driven telescope, tickmark distances are 8 arcsec and 8 min. The inclined Y-signal shows the decrease of the solar declination of $96''$ over two hours, the alomst horzontal X-signal reflects the finite accuracy of the tooth-wheel for the hour drive with 3–$4''$ amplitude and 4 min period.

5   Tests of the guider

The sensitivity of the sensor alone was tested operating the Locarno telescope exclusively with its hour drive and monitoring the output signals of the sensor. Fig. 3 shows that the Y-signal of the guider exactly follows the decrease of solar declination of $96''$ expected for August 15. The X-signal reflects the periodical 4 min motion introduced by the hour drive's 360-teeth-wheel which has a precision of about 1.5% yielding an amplitude of 3–$4''$. The rms fluctuations of these pure sensor signals are clearly below 1 arcsec.

In a second step, the combined sensor-telescope system was tested. For this purpose, the numerically converted guider signals were transmitted via a digital I/O card to the telescope motors. In order to avoid influences from the solar rotation on the test, a prominence footpoint on the (Hα) solar limb was monitored. Highest detectablility of possible drifts has been achieved using the new 'secondary image limb guider (cf. Sütterlin et al. 1997). The constant tilt angle of its glass plate being over several hours impressively proves the high guiding stability perpendicular to the limb. The other direction could be controlled via the (Hα) picture of the prominence.

In May 1997, the guider was attached to the Gregory telescope on Tenerife (Wiehr 1986). On May 23, an extended test was performed guiding a small sunspot 30" E-limb distance over as much as 11 h. The slit-jaw image was monitored with a CCD-camera
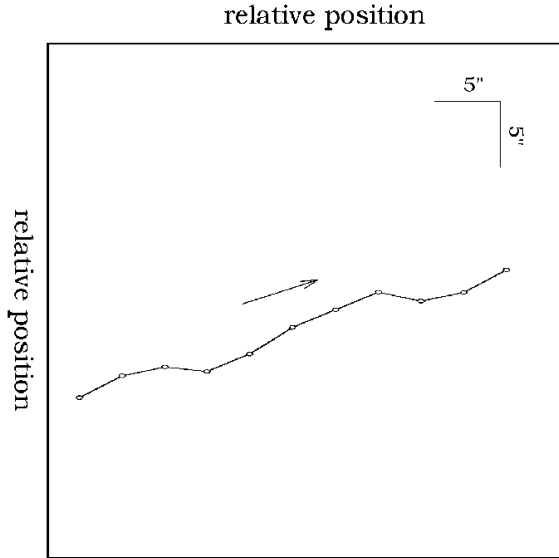
Figure 4: Residual motion of a sunspot near the solar limb under operation of the new primary image guider at the Gregory Coudé telescope on Tenerife; the ordinate gives the celestrial N-S, the abscissa the E-W direction, the arrow indicates the direction of rotation.

allowing a processing of the resulting images. In a first step, the Coudé rotation of $15°/h$ was removed. In a second step, the locations of sunspot and solar limb were determined with respect to the boundary of the telescope's secondary image, i.e. the rim of the pinhole in the prime focus.

The remaining spot migration, shown in Fig. 4, follows the solar rotation of $3.1''/h$ and the angle with the solar limb expected for that particular location on the solar disk. Remaining spatial deviations of less than $2''$ from the expected spot path may be caused by the reference system of the pinhole. The image of its rim is not perfectly round and shows two sharp segments, due to the $45°$ inclination of the field-stop with the telescope's optical axis. Furthermore, the guider monitors the primary image, whereas our measurements are done at the secondary image. Daily variations of the secondary imaging system can thus not be removed by our guider. The test demonstrates that our new guider does not yield the image drift up to 0.5 arcsec/min occuring with the old guider in the morning and evening hours. At steep telescope orientation near noon, the new guider at least performs as well as the old one.

The 'scanning mode' over small distances as e.g. $\pm100''$ yields a similar accuracy as the 'hold mode'. We expect influences by imaging errors from the guider optics only for a scan over large distances from the disk center, e.g. for a telescope pointing to given heliographic coordinates. Due to the simple optical components and the small f-number, spherical aberration, astigmatism and coma will cause an increasing

8

unsharpness when approaching the solar limb. Calculation of the geometrical spot diagrams shows that a maximal unsharpness of 4 arcsec (50% energy contour) will occur at 1000 arcsec distance from the optical axis (i.e. for solar limb observations). However, this effect can not affect the guiding 'stability' since the integral position of the sun is analyzed rather than the solar limb. The influences on the positioning accuracy, in turn, can be empirically determined and then corrected by the computer program.

6 Acknowledgment

References

[1] Bianda, M., Wiehr, E.: 1994, *Sterne & Weltraum* **33**, 108

[2] Blum, W., Kroha, H., Widmann, P.: 1995, 7th Europ. sympos. on Semiconductor detectors, Elmau casle

[3] Brückner, G., Schröter, E. H., Voigt, H. H.: 1967, *Solar Phys.* **1**, 4

[4] Küveler, G., Malchus, H., Zelano, F., Bianda, M.: 1994, *German Astron.Soc. abstract series* **10**, 244

[5] Soltau, D., Wiehr, E.: 1944, *Astron & Astrophys.* **141**, 159

[6] Sütterlin, P., Wiehr, E., Bianda, M., Küvelr, G.: 1997 *Astron & Astrophys.* **321**, 921

[7] Ten Bruggenkate, P., Jäger, F. W.: 1951, *Publ. Göttingen Obs*. **101**

[8] Wiehr, E., Wittmann, A., Wöhl, H.: 1980, *Solar Phys.* **68**, 207

[9] Wiehr E., 1986, in E. H. Schröter, M. Vazquez, A. A. Wyller (eds.), *The role of fine-scale magnetic fields on the structure of the solar photosphere*, p. 354